Submitted to Journal of American
Chemical Society

LBL-2324

REACTION PATHWAYS FOR THE TRIPLET METHYLENE ABSTRACTION $CH_2(^3B_1) + H_2 \rightarrow CH_3 + H$

Craig P. Baskin, Charles F. Bender,
Charles W. Bauschlicher Jr. and Henry F. Schaefer III

November 1973

Prepared for the U. S. Atomic Energy Commission
under Contract W-7405-ENG-48

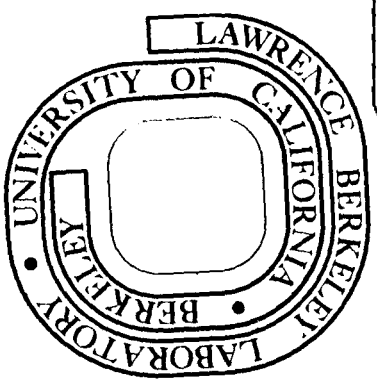

LBL-2324

DISCLAIMER

LBL-2324

Reaction Pathways for the Triplet Methylene Abstraction

$$CH_2(^3B_1) + H_2 \rightarrow CH_3 + H$$ [*]

by

Craig P. Baskin[**] and Charles F. Bender[***]

Lawrence Livermore Laboratory

University of California

Livermore, California 94550

and

Charles W. Bauschlicher Jr. and Henry F. Schaefer III[****]

Department of Chemistry and Lawrence Berkeley Laboratory

University of California

Berkeley, California 94720

[*] Work performed under the auspices of the U.S. Atomic Energy Commission.

[**] Present address: Department of Chemistry, University of California, Berkeley 94720

[***] M. H. Fellow.

[****] Alfred P. Sloan Fellow.

Abstract

A nonempirical quantum mechanical study of the reaction of triplet methylene with molecular hydrogen has been carried out. A contracted gaussian basis set of double zeta quality was employed. Following the determination of each self-consistent-field wave function, configuration interaction was performed including all singly-and doubly-excited configurations (a total of 649). The potential surface was studied in three dimensions and a total of 780 points computed. From these data, several approximations to the minimum energy path have been computed and compared. The reaction exothermicity is computed to be 5.37 kcal/mole, in good agreement with experiment, 4.5 kcal/mole. The predicted barrier height is 15.5 kcal/mole, a result consistent with the lack of any observed reaction between $CH_2(^3B_1)$ and H_2 at 300°K. The predicted barrier is 4.2 kcal/mole less than that obtained by Carr using the bond-energy bond-order (BEBO) method. The saddle point geometry is predicted to be

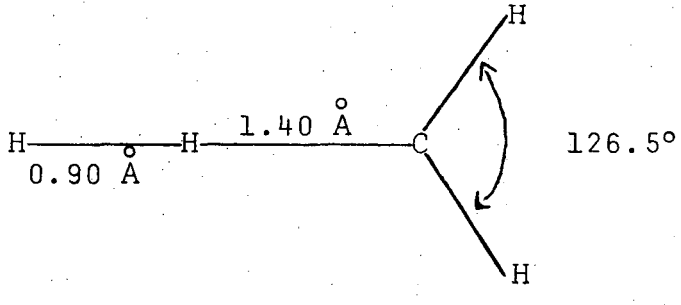

Introduction

Methylene reactions have become the topic of an increasing number of experimental[1-15] and theoretical[16-26] studies in recent years. And in fact the experimental studies have already yielded a wealth of valuable information about methylene reactions. For example, it now seems firmly established that triplet methylene abstracts hydrogen atoms from saturated hydrocarbons while the analogous reactions with singlet methylene yield insertion into CH bonds. One should note, however, that the interpretation of these experiments can be somewhat perilous. This is because in most cases the procedure used involves the photolysis of either ketene or diazomethane in the presence of the species with which a methylene reaction is desired. Although the elementary reactions of singlet and triplet methylene with the desired species will certainly occur to some degree, it is equally clear that a number of other chemical reactions may be taking place, e.g. the reaction of methylene with ketene to give ethylene and carbon monoxide. Ideally, one would like to be able to cross a beam of triplet or singlet methylenes with a beam of the other reactant, e.g. H_2. Even though a methylene crossed molecular beam experiment may sound unlikely, there does appear to be a real possibility[27] that such an experiment will be carried out within the next several years. The potential importance of experiments of this kind with respect to the discernment of the dynamics of methylene reactions can hardly be overemphasized.

In a similar manner, the theoretical studies of methylene reactions, while being something less than the ultimate, have significantly advanced our understanding of the chemistry of this short-lived intermediate. For example, both the extended Hückel calculations of Hoffmann[20] and the MINDO work of Dewar[25] have given strong support to the previously contested two-step mechanism of Benson[28] for the singlet methylene insertion into methane.

The prototype methylene reaction is $CH_2 + H_2$, hydrogen being the simplest partner molecule for which both abstraction and insertion reactions might occur. Among the several experimental studies[29-37] of this reaction, the most recent is that of Braun, Bass, and Pilling.[37] With rate constants at 298°K given in $cm^3/(molecule \cdot second)$, they summarize their results as follows:

$$CH_2(^1A_1) + H_2 \rightarrow CH_4^* \rightarrow CH_3 + H \qquad 7.0 \pm 1.5 \times 10^{-12} \qquad (1)$$

$$CH_2(^1A_1) + H_2 \rightarrow CH_2(^3B_1) + H_2 \qquad < 1.5 \times 10^{-12} \qquad (2)$$

$$CH_2(^3B_1) + H_2 \rightarrow CH_3 + H \qquad < 5.0 \times 10^{-14} \qquad (3)$$

In fact, Braun et.al. were unable to observe any reaction of triplet methylene with hydrogen at 300°K, and the figure given is an upper limit to the true rate constant. Recently Carr[22] has been able to rationalize this $^3B_1$ nonreactivity using Johnston and Parr's empirical bond-energy bond-order method[38] for the calculation of activation energies. Carr predicts the activation energy for $CH_2(^3B_1) + H_2 \rightarrow CH_3 + H$ to be quite high,

19.7 kcal/mole. Other computed abstraction activation energies ranged from 7.9 kcal/mole for C_3H_6 to 44.2 kcal/mole for HCN. It is worth noting that Dewar's predicted activation energy[25] of 3.8 kcal/mole for $CH_2(^3B_1) + CH_4 \rightarrow 2CH_3$ is qualitatively different from that of Carr, 25.6 kcal/mole.

Our ab initio theoretical study concerns the apparently slow $CH_2(^3B_1) + H_2$ abstraction reaction. The method used, which explicitly considers electron correlation, is analogous to that adopted in our previous study[39] of isolated CH_2. That study unequivocally predicted the nonlinearity of methylene at a time when a linear structure had been almost universally accepted. The two primary goals of the present study were a) to obtain a reliable (± 5 kcal/mole) prediction of the activation energy and b) to map out the minimum-energy-path for this simple reaction.

Theoretical Approach

A double zeta basis set of contracted gaussian functions[40] was used in the present work. For the carbon atom, Huzinaga's (9s 5p) primitive gaussian basis[41] was contracted to (4s 2p) following Dunning.[42] In analogous fashion a (4s/2s) basis was chosen for each H atom. The hydrogen basis functions were scaled by a factor of 1.2, i.e. each gaussian exponent α was multiplied by 1.44.

For C_{2v} approaches of the hydrogen molecule to $^3B_1$ methylene, the self-consistent-field (SCF) wave function is of the form

$$1a_1^2\ 2a_1^2\ 1b_2^2\ 3a_1^2\ 4a_1\ 1b_1 \qquad (4)$$

The SCF wave functions were obtained using a method recently developed by Davidson.[43] In addition we have computed configuration interaction wave functions which include all (except that the $1a_1$ orbital is always doubly occupied) singly-and doubly-excited configurations with respect to this SCF reference state. However, we have deleted those doubly-excited configurations which do not retain the open-shell spin coupling of the reference configuration. The deleted configurations i have identically zero Hamiltonian matrix elements H_{1i} with the SCF configuration.[44,45] A total of 649 configurations were included in the calculations.

Fortunately, the same SCF wave function (4) dissociates properly to SCF wave fundtions for the products CH_3 + H. Hence,

the true wave function should be reasonably well-described by a single configuration along the entire minimum energy path. This being the case, our single-and double-excitation CI should be nearly comparable (~95-98% of the correlation energy attainable from the chosen basis) to a full CI within the valence shell.[40] Three natural orbital iterations[46] were used in each calculation. Although in general such iterations tend to accelerate (lower total energy with fewer configurations) convergence of the CI expansion, the total energy was lowered relatively little (typically 0.003 hartrees) in the present cases, since the CI was initially nearly complete in a practical sense.

The accuracy of the potential surface should fall somewhere between that of our two surfaces[47,48] for F + H_2 → FH + H. Although the basis set here is analogous to that used in our preliminary study[47], a more thorough level of CI was used in the present study. Both the F + H_2 studies indicated the necessity of describing correlation effects in order to reliably predict the barrier height and exothermicity. Finally we note that the level of theory used in the present study seems[49] to predict equilibrium bond distances with a reliability of 0.03Å and bond angles to 2°.

Geometries Considered

Intuition suggests that the minimum-energy-path for CH_2 + H_2 should occur for a planar configuration in which the H-H molecule falls on the line bisecting the HCH methylene bond angle. However, Hoffmann has noted[50] that the surface may be rather flat with respect to a bending of the H_2 out of this plane. Such a C_{2v} reaction path is also the only path fully consistent with the MINDO results of Bodor, Dewar, and Wasson[25] for the analogous reaction $CH_2(^3B_1) + CH_4 \rightarrow 2\ CH_3$.

Therefore, we have restricted our study to the C_{2v} coordinate system shown in Figure 1. In addition, the two methylene CH distances have been frozen at 2.06 bohrs = 1.090 Å. The remaining geometrical parameters are a) R, the distance between the carbon atom and the closer of the two H atoms in H_2; b) r, the H-H separation in H_2; and c) θ, the methylene bond angle. As we go from reactants to products, these variables should change as follows:

$$
\begin{array}{lccc}
 & CH_2(^3B_1) + H_2 & \rightarrow & CH_3 + H \\
R & \infty & \rightarrow & \sim 1.08\ \text{Å} \\
r & 0.74\ \text{Å} & \rightarrow & \infty \\
\theta & \sim 134^\circ & \rightarrow & 120^\circ
\end{array}
\qquad (5)
$$

This three-dimensional potential surface has been determined at 780 points. The R values considered were 100.0, 10.0, 6.0,

5.0, 4.0, 3.0, 2.8, 2.6, 2.5, 2.4, 2.3, 2.2, 2.1, 2.06, and 2.0 bohrs. The H-H separation r took the values 1.2, 1.4, 1.6, 1.8, 2.0, 2.2, 2.4, 2.6, 2.8, 3.0, 3.2, 3.4, 3.6, 3.8, 4.0, 5.0, 6.0, 10.0 and 100.0 bohrs. Bond angles θ considered were 110°, 120°, 130°, and 140°. It is apparent that not all points on this 15 x 19 x 4 = 1140 point grid were computed. Many points which were clearly far from the minimum energy path were omitted. However, near the saddle point, a number of additional R values were used. The 780 computed total energies, in hartrees and kcal/mole relative to separated CH_2 + H_2, are given in the appendix to our complete report[51] of this research.

Table I summarizes our results for the reactants (separated $CH_2(^3B_1) + H_2$) and products (separated $CH_3 + H$). The former results were obtained at R = 100.0 bohrs and the latter at r = 100.0 bohrs.

The methylene bond angle is predicted to be 134.1°, which is nearly identical to the 134° value obtained from the best available theoretical calculation,[52] and consistent with experiment[53] 136 ± 5°. The predicted H_2 equilibrium separation is 0.007 Å longer than the exact result,[54] 0.7414 Å.

Although the two methylene CH distances were everywhere constrained to be 2.060 bohr = 1.090 Å, the third CH bond distance of the methyl radical is a variable, determined to be 1.094 Å. In addition, our calculations predict the methylene bond angle to be 120.2°. However, this bond angle is uncertain by perhaps 0.2° since the calculations were carried out at 10° intervals. Hence, although slightly unsymmetrical, our methyl radical structure is essentially the same as the planar experimental CD_3 structure of Herzberg[55] with r_o (CD) = 1.079 Å.

The reaction exothermicity is 0.00855 hartrees = 5.37 kcal/mole, in very good absolute agreement with the experimental value given by Carr,[22] 4.5 kcal/mole. The latter value is obtained from D_e (H-H) = 109.5 kcal/mole and D_e (CH_2-H) = 114.0 kcal/mole.

The saddle point or transition state[56] is the energetically highest point on a continuous path connecting $CH_2 + H_2$ with $CH_3 + H$. If several such points and paths occur, the true saddle

point for the reaction is that which is energetically lowest. The saddle point for our three-dimensional potential energy surface was located by using the stationary property

$$\frac{\partial E}{\partial R} = \frac{\partial E}{\partial r} = \frac{\partial E}{\partial \theta} = 0 \qquad (6)$$

With the obvious exception of the reactants, products and long range attractions, the predicted saddle point appears to be the only point on the ab initio surface which satisfies Eq. (6).

The predicted saddle point, seen in Figure 2, occurs at $R = 2.640$ bohrs $= 1.397$ Å, $r = 1.702$ bohrs $= 0.900$ Å, $\theta = 126.5°$. This geometry is intermediate between that of the products and reactants: the H-H separation is 0.152 Å or 20% longer than in H_2, while the H-C separation is 0.303 Å or 28% longer than in the isolated methyl radical. The fact that the transition state geometry is somewhat closer to the reactants than the products is consistent with Hammond's idea[57] that, in a highly exothermic reaction, the transition state should resemble the reactants.

The ab initio total energy at the saddle point is -40.10400 hartrees, which lies 15.5 kcal/mole above $CH_2(^3B_1) + H_2$. This 15.5 kcal/mole barrier does not, of course, reflect the zero-point vibrational energies of the reactants and transition state. The barrier height defined in this way is sometimes called the classical activation energy.[58] The Arrhenius activation energy for $CH_2(^3B_1) + H_2$ has not been measured, and the only related experimental information is the finding of Braun, Bass, and Pilling[37] that no reaction was observed at 300°K. Our 15.5 kcal/mole

barrier is sufficiently large to be consistent with their negative finding. As noted earlier, Carr[22] has used the empirical BEBO method to predict a barrier height of 19.7 kcal/mole. Although it is impossible to place error bars on our theoretical barrier height, based on earlier work,[46,47] we intuitively feel that the 15.5 kcal/mole result should be within 5 kcal/mole of the exact result. Thus our study gives further[59] evidence of the usefulness of the BEBO method. The only example we are familiar with in which BEBO fails seriously is the F + HF → FH + F reaction. There BEBO predicts a barrier of 6 kcal/mole,[60] while the best ab initio calculations[61] imply a barrier ≥ 18 kcal/mole.

On the basis of our earlier work on the radical plus diatom reactions[47,48,61,62] F + H_2, H + F_2, and F + HF, we were skeptical of the ability of single configuration SCF wave functions to describe the $CH_2(^3B_1)$ + H_2 potential surface. However, from a theoretical point of view, any information on the suitability of the Hartree-Fock approximation with respect to such reactions is extremely valuable. Therefore the relative energies and geometries of the reactants, saddle point and products were obtained from the SCF potential surface. The calculated exothermicity for $CH_2(^3B_1)$ + H_2 → CH_3 + H was found to be 4.84 kcal/mole, which is actually in somewhat better agreement with experiment,[21] ~ 4.5 kcal/mole, than the CI result, 5.37 kcal/mole. However, the barrier height is computed to be 25.1 kcal/mole, or 9.6 kcal/mole higher than

the CI result. Although the barrier height is not known experimentally, our previous experience[47,48,61,62] would suggest that it may be close to or slightly lower than the CI result, and hence that the SCF barrier may be much too high. The SCF saddle point geometry is R = 2.53 bohrs, r = 1.69 bohrs, θ = 124.8°. Thus the SCF and CI transition state geometries are quite similar, much more so than was the case[46,47,61] for F + H_2 and H + F_2.

Reaction Pathways

In both textbooks and the literature, one frequently finds terms such as "reaction coordinate", "reaction path", "path of least energy", and "minimum energy path" used interchangeably. We find this situation unfortunate, since there are at least two distinct procedures by which such a path might be obtained.

The most frequently used procedure is to choose a "reaction coordinate", some geometrical parameter that varies significantly during the course of reaction. For the $CH_2(^3B_1) + H_2$ reaction, either R (which goes from ∞ to 1.094 Å) or r (which goes from 0.748 Å to ∞) would be reasonable choices. θ, which goes from 134° to 120°, would probably not be a very good choice, since it does not undergo a large change during the reaction. Given a value of the "reaction coordinate", one finds a point on the "reaction path" by minimizing the total energy with respect to all other geometrical parameters.[63] Hereafter, our use of the terms "reaction coordinate" and "reaction path" will be strictly as defined above.

Under favorable conditions, a reaction coordinate will vary monotonically along the reaction path, and the energetically highest point on the reaction path will occur near the true saddle point. However, there are many exceptions to this favorable behavior, an especially interesting example being the MINDO treatment of the interconversion of cyclobutene and butadiene.[64] Even if a reaction path does pass close by the saddle point,

there are situations in which the reaction path will appear unrealistic. These situations generally occur when a small change in the chosen reaction coordinate is accompanied by large changes in other geometrical parameters. One example of such behavior is noted by Dobson, Hayes, and Hoffmann[20] in their study of $CH_2(^1A_1) + CH_4$.

There is at least one procedure[47,56] which defines the reaction pathway (an intentionally vague term) in a far more satisfactory manner. Rather than starting from either reactants or products, this procedure begins with the saddle point. From the saddle point, one follows the gradient $\vec{\nabla} V$ of the potential energy in the direction of most negative curvature. Following the gradient leads in one direction to reactants and in the other direction to products, and we refer to the resulting path between products and reactants as the "minimum energy path". Note that although this definition is dependent on choice of coordinate system, one expects such dependence to be in general unimportant.

Table II gives the reaction path for reaction coordinate R, the reaction path for reaction coordinate r, and the minimum energy path. Let us first describe the "minimum energy path", since this is the mathematical embodiment of what the chemist visualizes as the reaction pathway. Along the minimum energy path, all three variables R, r, and θ vary smoothly. On the reactants side, prior to R = 3.0, R is changing rapidly relative to the rather small changes in r and θ. Around the saddle point,

say between R = 3.0 and r = 2.0, all three geometrical parameters are changing significantly. Finally, from r = 2.0 to r = 100, small changes in R and θ accompany large changes in r.

Inspection of Table II makes it quite apparent that the choice of R as a reaction coordinate is appropriate for the reactant side of the minimum energy path, but not for the product side. The problem is that the value of r lurches from 1.756 to 6.0 as R changes from 2.6 to 2.5. As the minimum energy path shows, the "correct" value of r for R = 2.5 is ~ 1.81 bohrs.

An opposite, but even more serious, breakdown occurs with respect to the choice of r as reaction coordinate. That is, on the product side (r > 2.0 bohrs), the reaction path obtained using r as reaction coordinate is quite similar to the minimum energy path. However, this reaction path also lurches, between r = 1.9 and 1.8, and is inapplicable on the reactants side of the saddle point. Hence the saddle point position is not correctly predicted. In fact, inspection of Table II would suggest that we have found a lower energy (~ 13 kcal barrier) route from $CH_2 + H_2$ to $CH_3 + H$. The problem lies with the discontinuous change of R and θ along this reaction path.

Recall that a point on the above reaction path is obtained, for a particular value of r, by minimizing the total energy with respect to R and θ. Unfortunately, when r is in the range 1.6 - 1.9 bohrs, there are two distinct relative minima. The first occurs for R ≈ 2.3 bohrs, θ ≈ 123° and the second for R ≈ 6.0

bohrs, $\theta \approx 134°$. When r is greater than 1.84 bohrs, the first minima is the lower, but for $r < 1.84$, the second minima is lower. At r = 1.84 the two minima both have depth 13.59 kcal/mole, as illustrated in Figure 3. Hence the reaction path based on r as reaction coordinate has a discontinuity at r = 1.84. This gives the mistaken impression that the barrier height is 13.59 kcal/mole. In fact, as Figure 3 shows, a continuous reaction path between r = 1.841 and r = 1.839 would have to pass over a barrier of 18.50 kcal/mole.

If one must choose a reaction coordinate, a reasonable choice is (r - R), which changes in a fairly smooth manner all along the minimum energy path. Although this conclusion is by no means unanticipated, the quantitative analysis made possible by Table II seems to be of considerable value.

Concluding Remarks

The barrier height for the $CH_2(^3B_1) + H_2 \rightarrow CH_3 + H$ reaction has been predicted ab initio to be 15.5 kcal/mole. This result will probably come as a surprise to those who have pictured methylene as an extremely reactive radical. The concept of reaction pathway has been discussed, emphasizing the importance of the minimum energy path.

Acknowledgments

We thank Professors Don Bunker and Roald Hoffmann for helpful discussions. This research was supported by the National Science Foundation, Grant GP - 31974.

References

1. H. M. Frey, Prog. React. Kinet. 2, 131 (1964).
2. Experimental references prior to 1971 are given by W. Kirmse, Carbene Chemistry (Academic Press, New York, 1971).
3. D. C. Montague and F. S. Rowland, J. Amer. Chem. Soc. 93, 5381 (1971); Chem. Comm. 193 (1972).
4. H. D. Roth, J. Amer. Chem. Soc. 93, 1527, 4935 (1971); 94, 1400, 1761 (1972).
5. J. A. Bell, J. Phys. Chem. 75, 1537 (1971).
6. K. Dee, D. W. Setser and W. G. Clark, J. Phys. Chem. 75, 2231, 2240 (1971).
7. P. Boldt, W. Thielecke, and H. Luthe, Chem. Ber. 104, 353 (1971).
8. G. W. Taylor and J. W. Simons, Int. J. Chem. Kinet. 3, 25 (1971); W. L. Hase and J. W. Simons, J. Organometal. Chem. 32, 47 (1971); J. Chem. Phys. 54, 1277 (1971); W. L. Hase, R. J. Phillips, and J. W. Simons, Chem. Phys. Lett. 12, 161 (1971); W. L. Hase, R. L. Johnson, and J. W. Simons, Int. J. Chem. Kinet. 4, 1 (1972); F. B. Growcock, W. L. Hase and J. W. Simons, J. Phys. Chem. 76, 607 (1972).
9. J. R. McNesby and R. V. Kelly, Int. J. Chem. Kinet. 3, 293 (1971).
10. R. E. Rebbert, S. G. Lias, and P. Ausloos, Chem. Phys. Lett. 12, 323 (1971).
11. R. W. Hoffmann, Angew. Chem. Int. Ed. Engl. 10, 529 (1971).

12. D. Seyferth and C. K. Haas, J. Organometal. Chem. 39, C33 (1972).

13. R. T. Conlin, P. P. Gaspar, R. H. Levin, and M. Jones, J. Amer. Chem. Soc. 94, 7165 (1972).

14. M. Pomerantz, A. S. Ross, and G. W. Gruber, J. Amer. Chem. Soc. 94, 1403 (1972).

15. G. B. Kistiakowsky and B. B. Saunders, J. Phys. Chem. 77, 427 (1973).

16. P. S. Skell, S. J. Valenty, and P. W. Humer, J. Amer. Chem. Soc. 95, 5041 (1973).

17. R. Hoffmann, J. Amer. Chem. Soc. 90, 1475 (1968).

18. H. Kollmar, Tetrahedron Letters 3337 (1970).

19. R. Hoffmann, R. Gleiter, and F. B. Mallory, J. Amer. Chem. Soc. 92, 1460 (1970).

20. R. C. Dobson, D. M. Hayes, and R. Hoffmann, J. Amer. Chem. Soc. 93, 6188 (1971).

21. H. Basch, J. Chem. Phys. 55, 1700 (1971).

22. R. W. Carr, J. Phys. Chem. 76, 1581 (1972).

23. H. Kollmar, Tetrahedron 28, 5893 (1972).

24. H. Fujimoto, S. Yamabe, and K. Fujui, Bull. Chem. Soc. Japan 45, 2424 (1972).

25. N. Bodor, M. J. S. Dewar, and J. S. Wasson, J. Amer. Chem. Soc. 94, 9095 (1972).

26. N. Bodor and M. J. S. Dewar, J. Amer. Chem. Soc. 94, 9103 (1973).

27. D. R. Herschbach, personal communication.

28. S. W. Benson, Advan. Photochem. 2, 1 (1964); W. B. Moore and S. W. Benson, ibid., 2, 219 (1964).

29. F. W. Kirkbride and R. G. W. Norrish, J. Chem. Soc. (London) 119 (1933).

30. C. Rosenblum, J. Amer. Chem. Soc. 60, 2819 (1938); 63, 3322 (1941).

31. C. E. H. Bawn and J. Milstead, Trans. Faraday Soc. 35, 889 (1939).

32. H. Wiener and M. Burton, J. Amer. Chem. Soc. 75, 5815 (1953).

33. J. Chanmugam and M. Burton, J. Amer. Chem. Soc. 78, 509 (1956); Can. J. Chem. 34, 1021 (1956).

34. H. Gesser and E. W. R. Steacie, Can. J. Chem. 34, 113 (1956).

35. G. Herzberg, Proc. Roy. Soc. (London), A 262, 291 (1961).

36. J. A. Bell and G. B. Kistiakowsky, J. Amer. Chem. Soc. 84, 3417 (1962).

37. W. Braun, A. M. Bass, and M. Pilling, J. Chem. Phys. 52, 5131 (1970).

38. H. S. Johnston and C. Parr, J. Amer. Chem. Soc. 85, 2544 (1963).

39. C. F. Bender and H. F. Schaefer, J. Amer. Chem. Soc. 92, 4984 (1970).

40. H. F. Schaefer, The Electronic Structure of Atoms and Molecules: A Survey of Rigorous Quantum Mechanical Results (Addison-Wesley, Reading, Massachusetts, 1972).

41. S. Huzinaga, J. Chem. Phys. 42, 1293 (1965).

42. T. H. Dunning, J. Chem. Phys. 53, 2823 (1970).

43. E. R. Davidson, to be published.

44. A. Bunge, J. Chem. Phys. 53, 20 (1970).

45. A. D. McLean and B. Liu, J. Chem. Phys. 58, 1066 (1973).

46. C. F. Bender and E. R. Davidson, J. Phys. Chem. 70, 2675 (1966).

47. C. F. Bender, P. K. Pearson, S. V. O'Neil, and H. F. Schaefer, J. Chem. Phys. 56, 4626 (1972).

48. C. F. Bender, S. V. O'Neil, P. K. Pearson, and H. F. Schaefer, Science 176, 1412 (1972).

49. H. F. Schaefer, "Status of Ab Initio Molecular Structure Predictions," Advances in Chemistry, in press.

50. R. Hoffmann, personal communication.

51. C. P. Baskin. C. F. Bender, C. W. Bauschlicher, and H. F. Schaefer, Lawrence Berkeley Laboratory Report No. LBL-0000, November, 1973.

52. D. R. McLaughlin, C. F. Bender, and H. F. Schaefer, Theoret. Chim. Acta 25, 352 (1972).

53. G. Herzberg and J. W. C. Johns, J. Chem. Phys. 54, 2276 (1971); E. Wasserman, V. J. Kuck, R. S. Hutton, E. D. Anderson, and W. A. Yager, J. Chem. Phys. 54, 4120 (1971).

54. W. Kolos and L. Wolniewicz, J. Chem. Phys. 49, 404 (1968).

55. G. Herzberg, Electronic Spectra of Polyatomic Molecules (Van Nostrand Reinhold, New York, 1966).

56. For a clear discussion, see J. W. McIver and A. Komornicki, Chem. Phys. Lett., 10, 303 (1971); J. Amer. Chem. Soc. 94, 2625 (1972).

57. G. S. Hammond, J. Am. Chem. Soc. 77, 334 (1955).

58. M. Karplus, page 378 in Molecular Beams and Reaction Kinetics, edited by Ch. Schlier (Academic Press, New York, 1970).

59. D. G. Truhlar, J. Am. Chem. Soc. 94, 7584 (1972).

60. H. S. Johnston, Gas Phase Reaction Rate Theory (Ronald Press, New York, 1966).

61. S. V. O'Neil, H. F. Schaefer, and C. F. Bender, Proc. Natl. Acad. Sci. U. S. A. in press.

62. S. V. O'Neil, P. K. Pearson, H. F. Schaefer, and C. F. Bender, J. Chem. Phys. 58, 1126 (1973).

63. P. B. Empedocles, Int. J. Quantum Chem. 3S, 47 (1969).

64. M. J. S. Dewar and S. Kirschner, J. Am. Chem. Soc. 93, 4292 (1971).

Table I. Geometries and total energies of reactants and products.

$\underline{CH_2(^3B_1) + H_2}$

E = -40.12866 hartrees

r (CH) = 1.090 Å (assumed)

θ (HCH) = 134.1°

r (HH) = 0.748 Å

$\underline{CH_3 + H}$

E = -40.13722 hartrees

r (CH) = 1.094 Å

θ (HCH) = 120.2°

Table II. Reaction paths for $CH_2(^3B_1) + H_2 \rightarrow CH_3 + H$. Bond distances are in bohr radii, bond angles in degrees and energies in kcal/mole.

Minimum Energy Path				R Reaction Coordinate				r Reaction Coordinate			
R	r	θ	E	R	r	θ	E	R	r	θ	E
100.0	1.414	134.1	0.00	100.0	1.414	134.1	0.00	6.0	1.4	134.1	-0.02
6.0	1.412	134.1	-0.04	6.0	1.412	134.1	-0.04				
5.0	1.412	133.9	0.50	5.0	1.412	133.9	0.50				
4.5	1.412	133.8	1.35	4.5	1.412	133.8	1.35				
4.0	1.420	133.3	3.39	4.0	1.420	133.3	3.39				
3.8	1.428	132.9	4.66	3.8	1.428	132.9	4.66				
3.6	1.440	132.4	6.22	3.6	1.440	132.4	6.22				
3.4	1.452	131.9	8.05	3.4	1.452	131.9	8.05				
3.2	1.468	131.2	10.27	3.2	1.468	131.2	10.27				
3.0	1.524	130.0	12.72	3.0	1.504	130.0	12.63	6.0	1.5	134.1	0.81
2.8	1.612	128.1	14.82	2.8	1.572	128.2	14.70				
2.7	1.660	127.2	15.35	2.7	1.640	127.2	15.35	6.0	1.6	134.1	3.40
2.640	1.702	126.5	15.48	2.65	1.692	126.6	15.48	6.0	1.7	134.1	7.13
2.514	1.80	125.2	14.92	2.6	1.756	126.0	15.41	6.0	1.8	134.1	11.64
2.394	1.90	123.5	13.23	2.5	6.0	123.6	8.52	2.268	1.9	122.6	12.57
2.301	2.0	122.4	11.28	2.4	6.0	122.6	3.64	2.175	2.0	122.0	10.87
2.198	2.2	121.6	7.89	2.3	6.0	122.0	-0.54	2.155	2.2	121.3	7.68
2.140	2.4	120.9	4.82	2.2	6.0	121.3	-3.66	2.125	2.4	120.9	4.87
2.110	2.6	120.6	2.52	2.1	6.0	120.5	-5.29	2.103	2.6	120.6	2.54
2.095	2.8	120.4	0.63					2.090	2.8	120.3	0.63
2.085	3.0	120.3	-0.89					2.083	3.0	120.3	-0.89
2.073	3.5	120.2	-3.37					2.073	3.5	120.2	-3.37
2.068	4.0	120.2	-4.58					2.068	4.0	120.2	-4.58
2.068	5.0	120.2	-5.33					2.068	5.0	120.2	-5.33
2.068	6.0	120.2	-5.41	2.06	6.0	120.2	-5.40	2.068	6.0	120.2	-5.41
2.068	100.0	120.2	-5.37					2.068	100.0	120.2	-5.37

Figure Captions

Fig. 1 Coordinate system for $CH_2(^3B_1) + H_2 \rightarrow CH_3 + H$.

Fig. 2 Transition state geometry for $CH_2(^3B_1) + H_2 \rightarrow CH_3 + H$.

Fig. 3 Illustration of the discontinuity of the reaction path obtained by choosing r as reaction coordinate. Each point on the curve corresponds to the value of R shown on the x-axis, r = 1.84 bohrs, and the value of θ for which the potential energy is minimized.

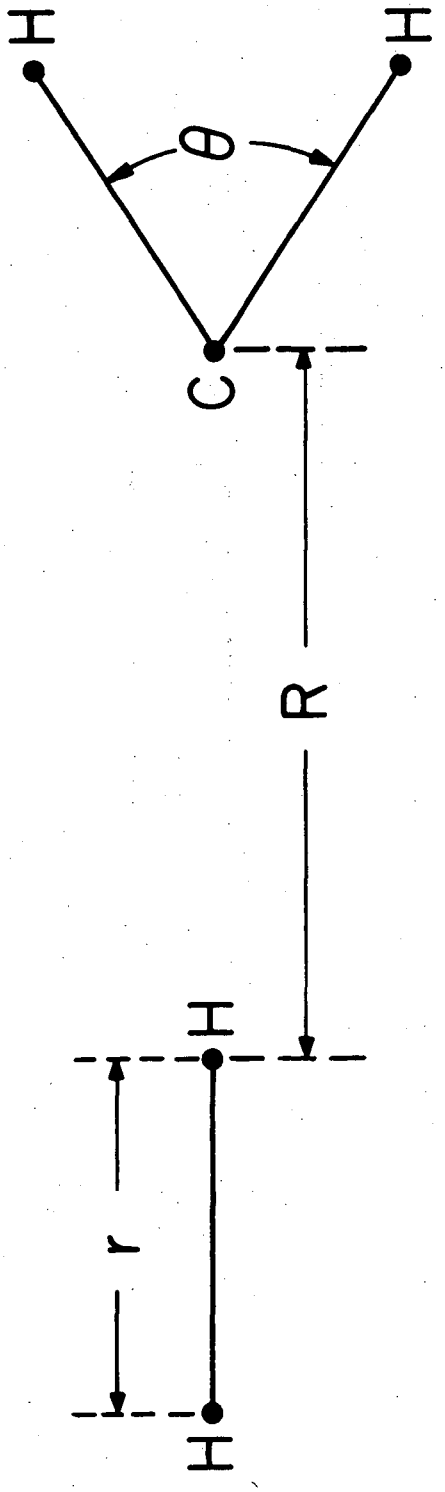

XBL739-4044

Fig. 1

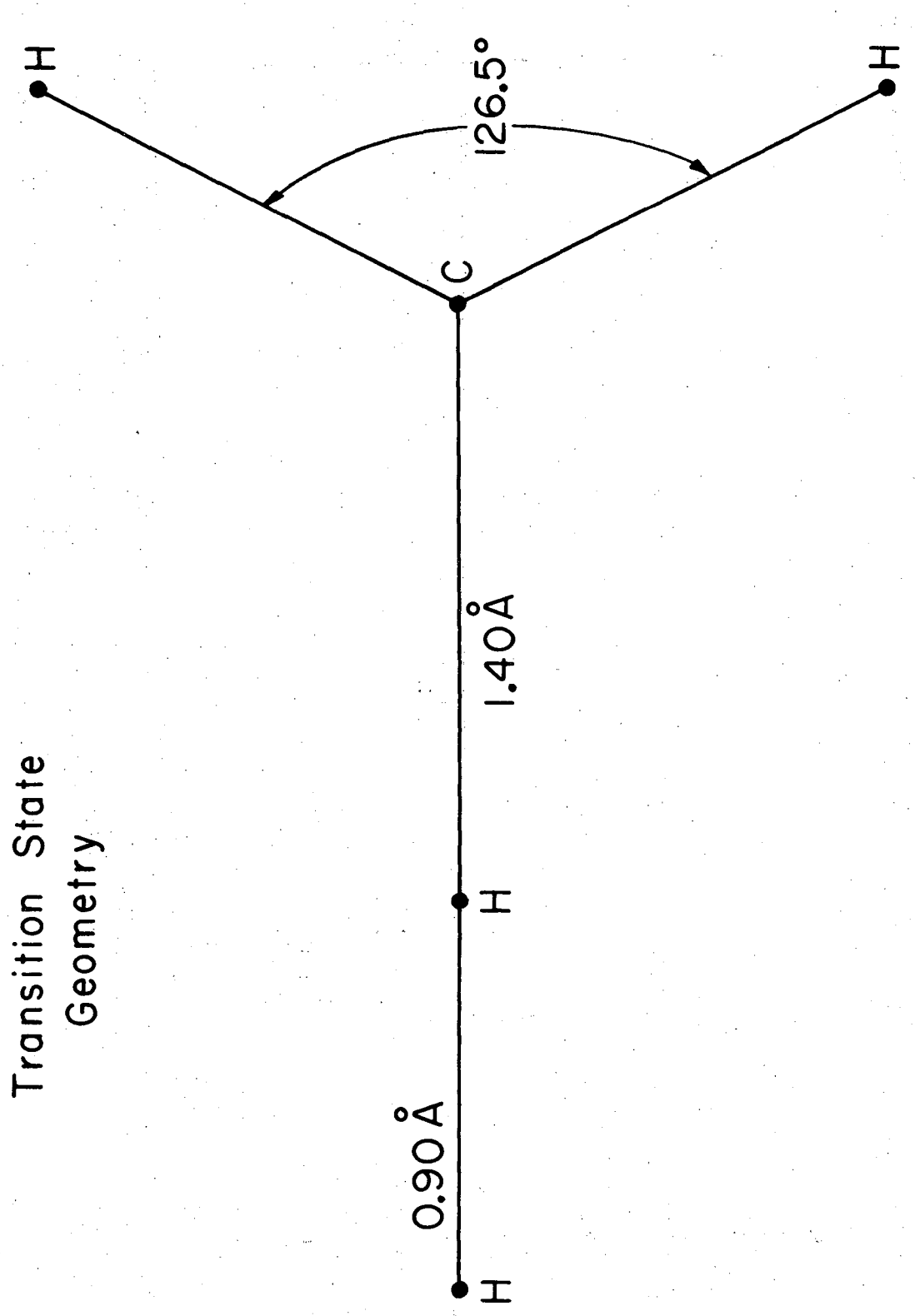
H
126.5°
H
C
1.40Å
H
0.90Å
H
Transition State
Geometry
XBL7310-4295

Fig. 2

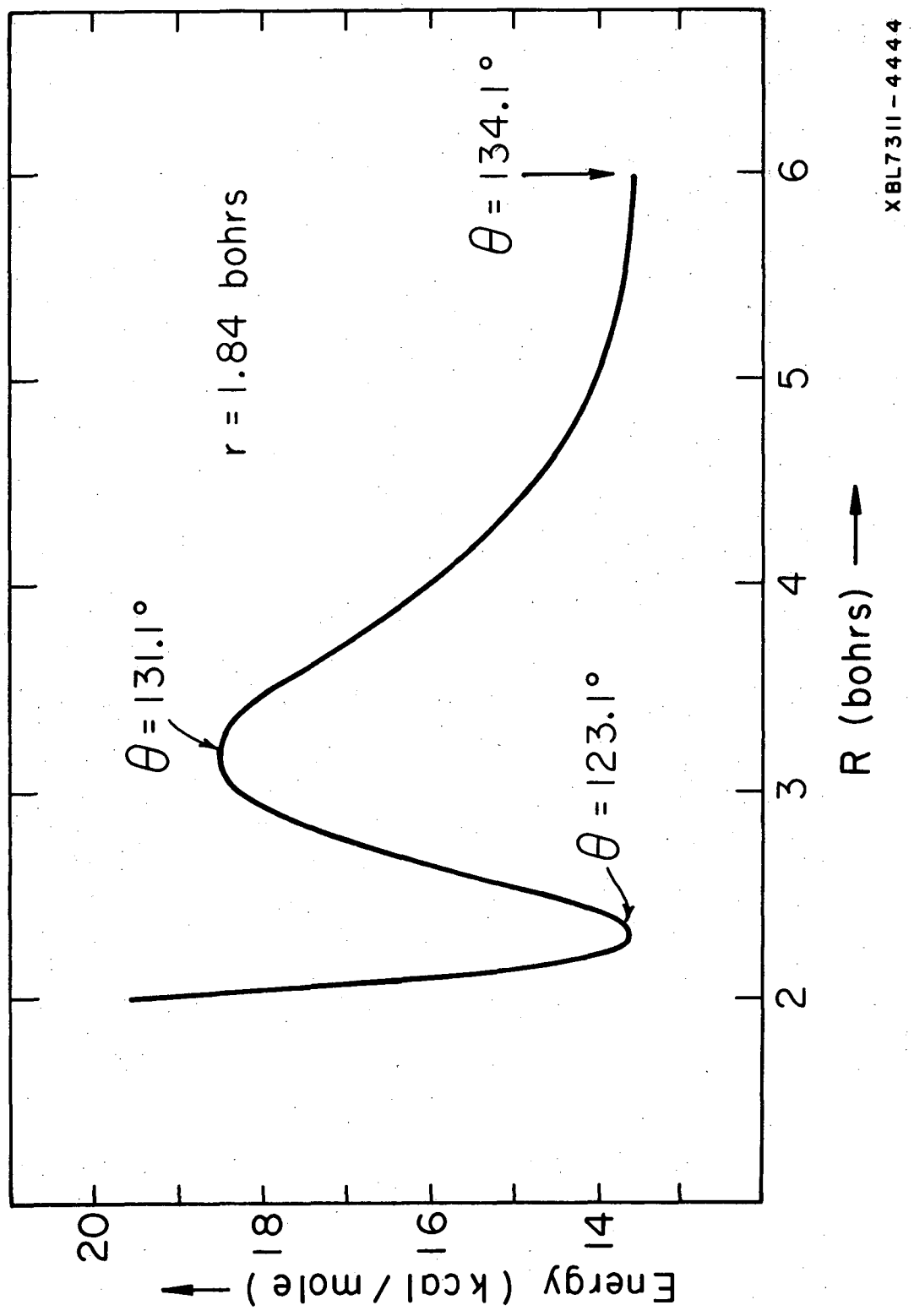
r = 1.84 bohrs
θ = 131.1°
θ = 123.1°
θ = 134.1°
Energy (kcal / mole)
R (bohrs)
20
18
16
14
2
3
4
5
6
XBL7311-4444

Fig. 3

Appendix

ANGLE	RCH	RHH	E	E(KCAL/MOLE)
110	100.000	1.200	-40.108643	12.566171
120	100.000	1.200	-40.115269	8.408356
130	100.000	1.200	-40.118035	6.672691
140	100.000	1.200	-40.117771	6.838351
110	100.000	1.400	-40.118986	6.075938
120	100.000	1.400	-40.125610	1.919378
130	100.000	1.400	-40.128372	.186223
140	100.000	1.400	-40.128102	.355648
110	100.000	1.600	-40.113500	9.518403
120	100.000	1.600	-40.120122	5.363098
130	100.000	1.600	-40.122879	3.633081
140	100.000	1.600	-40.122599	3.808781
110	100.000	1.800	-40.100345	17.773166
120	100.000	1.800	-40.106963	13.620371
130	100.000	1.800	-40.109712	11.895373
140	100.000	1.800	-40.109422	12.077348
110	10.000	1.200	-40.108662	12.554248
120	10.000	1.200	-40.115290	8.395178
130	10.000	1.200	-40.118058	6.658258
140	10.000	1.200	-40.117796	6.822663
110	10.000	1.400	-40.119009	6.061506
120	10.000	1.400	-40.125635	1.903691
130	10.000	1.400	-40.128400	.168653
140	10.000	1.400	-40.128131	.337451
110	10.000	1.600	-40.113527	9.501461
120	10.000	1.600	-40.120152	5.344273
130	10.000	1.600	-40.122911	3.613001
140	10.000	1.600	-40.122634	3.786816
110	10.000	1.800	-40.100376	17.753713
120	10.000	1.800	-40.106997	13.599036
130	10.000	1.800	-40.109749	11.872156
140	10.000	1.800	-40.109461	12.052876
110	6.000	1.200	-40.108717	12.519736
120	6.000	1.200	-40.115327	8.371961
130	6.000	1.200	-40.118075	6.647591
140	6.000	1.200	-40.117794	6.823918
110	6.000	1.400	-40.119086	6.013188
120	6.000	1.400	-40.125700	1.862903
130	6.000	1.400	-40.128452	.136023
140	6.000	1.400	-40.128171	.312351
110	6.000	1.600	-40.113627	9.438711
120	6.000	1.600	-40.120245	5.285916
130	6.000	1.600	-40.122998	3.558408
140	6.000	1.600	-40.122715	3.735991
110	6.000	1.800	-40.100497	17.677786
120	6.000	1.800	-40.107117	13.523736
130	6.000	1.800	-40.109868	11.797483
140	6.000	1.800	-40.109581	11.977576
110	6.000	2.000	-40.084007	28.025261
120	6.000	2.000	-40.090627	23.871211
130	6.000	2.000	-40.093374	22.147468
140	6.000	2.000	-40.093078	22.333208
110	6.000	2.200	-40.066484	39.020943
120	6.000	2.200	-40.073101	34.868776
130	6.000	2.200	-40.075841	33.149426

140	6.000	2.200	-40.075532	33.343323
110	5.000	1.200	-40.107915	13.022991
120	5.000	1.200	-40.114467	8.911611
130	5.000	1.200	-40.117153	7.226146
140	5.000	1.200	-40.116809	7.442006
110	5.000	1.400	-40.118347	6.476911
120	5.000	1.400	-40.124914	2.356118
130	5.000	1.400	-40.127615	.661241
140	5.000	1.400	-40.127284	.868943
110	5.000	1.600	-40.112956	9.859763
120	5.000	1.600	-40.119538	5.729558
130	5.000	1.600	-40.122251	4.027151
140	5.000	1.600	-40.121932	4.227323
110	5.000	1.800	-40.099892	18.057423
120	5.000	1.800	-40.106485	13.920316
130	5.000	1.800	-40.109210	12.210378
140	5.000	1.800	-40.108898	12.406158
110	5.000	2.000	-40.083463	28.366621
120	5.000	2.000	-40.090066	24.223238
130	5.000	2.000	-40.092799	22.508261
140	5.000	2.000	-40.092490	22.702178
110	5.000	2.200	-40.065995	39.327791
120	5.000	2.200	-40.072604	35.180643
130	5.000	2.200	-40.075340	33.463803
140	5.000	2.200	-40.075028	33.659583
110	4.000	1.200	-40.103155	16.009891
120	4.000	1.200	-40.109472	12.045973
130	4.000	1.200	-40.111929	10.504206
140	4.000	1.200	-40.111363	10.859371
110	4.000	1.400	-40.114142	9.115548
120	4.000	1.400	-40.120512	5.118373
130	4.000	1.400	-40.123020	3.544603
140	4.000	1.400	-40.122498	3.872158
110	4.000	1.600	-40.109343	12.126921
120	4.000	1.600	-40.115763	8.098371
130	4.000	1.600	-40.118321	6.493226
140	4.000	1.600	-40.117843	6.793171
110	4.000	1.800	-40.096907	19.930511
120	4.000	1.800	-40.103373	15.873096
130	4.000	1.800	-40.105977	14.239086
140	4.000	1.800	-40.105538	14.514558
110	4.000	2.000	-40.081145	29.821166
120	4.000	2.000	-40.087654	25.736768
130	4.000	2.000	-40.090298	24.077658
140	4.000	2.000	-40.089890	24.333678
110	4.000	2.200	-40.064398	40.329908
120	4.000	2.200	-40.070942	36.223548
130	4.000	2.200	-40.073618	34.544358
140	4.000	2.200	-40.073234	34.785318
110	3.000	1.200	-40.084365	27.800616
120	3.000	1.200	-40.089633	24.494946
130	3.000	1.200	-40.091045	23.608916
140	3.000	1.200	-40.089389	24.648056
110	3.000	1.400	-40.100032	17.969573
120	3.000	1.400	-40.105410	14.594878
130	3.000	1.400	-40.106910	13.653628

140	3.000	1.400	-40.105302	14.662648
110	3.000	1.600	-40.100520	17.663353
120	3.000	1.600	-40.105901	14.286776
130	3.000	1.600	-40.107539	13.258931
140	3.000	1.600	-40.105945	14.259166
110	3.000	1.800	-40.094146	21.663038
120	3.000	1.800	-40.099649	18.209906
130	3.000	1.800	-40.101221	17.223476
140	3.000	1.800	-40.099591	18.246301
110	3.000	2.000	-40.085487	27.096561
120	3.000	2.000	-40.090974	23.653468
130	3.000	2.000	-40.092495	22.699041
140	3.000	2.000	-40.090755	23.790891
110	3.000	2.200	-40.077208	32.291633
120	3.000	2.200	-40.082621	28.894976
130	3.000	2.200	-40.084024	28.014593
140	3.000	2.200	-40.082102	29.220648
110	2.800	1.200	-40.077336	32.211313
120	2.800	1.200	-40.082145	29.193666
130	2.800	1.200	-40.083080	28.606953
140	2.800	1.200	-40.080900	29.974903
110	2.800	1.400	-40.095647	20.721161
120	2.800	1.400	-40.100568	17.633233
130	2.800	1.400	-40.101581	16.997576
140	2.800	1.400	-40.099422	18.352348
110	2.800	1.600	-40.099103	18.552521
120	2.800	1.600	-40.104092	15.421923
130	2.800	1.600	-40.105134	14.768068
140	2.800	1.600	-40.102941	16.144176
110	2.800	1.800	-40.096063	20.460121
120	2.800	1.800	-40.101056	17.327013
130	2.800	1.800	-40.102058	16.698258
140	2.800	1.800	-40.099755	18.143391
110	2.800	2.000	-40.091055	23.602641
120	2.800	2.000	-40.095990	20.505928
130	2.800	2.000	-40.096883	19.945571
140	2.800	2.000	-40.094396	21.506163
110	2.800	2.200	-40.086515	26.451491
120	2.800	2.200	-40.091342	23.422548
130	2.800	2.200	-40.092073	22.963846
140	2.800	2.200	-40.089346	24.675038
110	2.700	1.200	-40.073195	34.809791
120	2.700	1.200	-40.077733	31.962196
130	2.700	1.200	-40.078407	31.539261
140	2.700	1.200	-40.075883	33.123071
110	2.700	1.400	-40.093208	22.251633
120	2.700	1.400	-40.097859	19.333131
130	2.700	1.400	-40.098578	18.881958
140	2.700	1.400	-40.096082	20.448198
110	2.700	1.600	-40.098529	18.912706
120	2.700	1.600	-40.103237	15.958436
130	2.700	1.600	-40.103967	15.500361
140	2.700	1.600	-40.101408	17.106133
110	2.700	1.800	-40.097490	19.564678
120	2.700	1.800	-40.102186	16.617938
130	2.700	1.800	-40.102850	16.201278

140	2.700	1.800	-40.100148	17.896783
110	2.700	2.000	-40.094508	21.435883
120	2.700	2.000	-40.099129	18.536206
130	2.700	2.000	-40.099662	18.201748
140	2.700	2.000	-40.096737	20.037186
110	2.675	1.200	-40.072081	35.508826
120	2.675	1.200	-40.076548	32.705783
130	2.675	1.200	-40.077120	32.346853
140	2.675	1.200	-40.074535	33.968941
110	2.675	1.400	-40.092563	22.656371
120	2.675	1.400	-40.097143	19.782421
130	2.675	1.400	-40.097784	19.380193
140	2.675	1.400	-40.095197	21.003536
110	2.675	1.600	-40.098391	18.999301
120	2.675	1.600	-40.103024	16.092093
130	2.675	1.600	-40.103671	15.686101
140	2.675	1.600	-40.101014	17.353368
110	2.675	1.700	-40.098589	18.875056
120	2.675	1.700	-40.103223	15.967221
130	2.675	1.700	-40.103843	15.578171
140	2.675	1.700	-40.101119	17.287481
110	2.675	1.800	-40.097879	19.320581
120	2.675	1.800	-40.102496	16.423413
130	2.675	1.800	-40.103072	16.061973
140	2.675	1.800	-40.100265	17.823366
110	2.675	2.000	-40.095413	20.867996
120	2.675	2.000	-40.099955	18.017891
130	2.675	2.000	-40.100395	17.741791
140	2.675	2.000	-40.097352	19.651273
110	2.650	1.200	-40.070933	36.229196
120	2.650	1.200	-40.075327	33.471961
130	2.650	1.200	-40.075820	33.162603
140	2.650	1.200	-40.073148	34.839283
110	2.650	1.400	-40.091902	23.071148
120	2.650	1.400	-40.096408	20.243633
130	2.650	1.400	-40.096969	19.891606
140	2.650	1.400	-40.094289	21.573306
110	2.650	1.600	-40.098252	19.086523
120	2.650	1.600	-40.102808	16.227633
130	2.650	1.600	-40.103370	15.874978
140	2.650	1.600	-40.100613	17.604996
110	2.650	1.700	-40.098718	18.794108
120	2.650	1.700	-40.103275	15.934591
130	2.650	1.700	-40.103807	15.600761
140	2.650	1.700	-40.100979	17.375331
110	2.650	1.800	-40.098275	19.072091
120	2.650	1.800	-40.102815	16.223241
130	2.650	1.800	-40.103301	15.918276
140	2.650	1.800	-40.100386	17.747438
110	2.650	2.000	-40.096327	20.294461
120	2.650	2.000	-40.100789	17.494556
130	2.650	2.000	-40.101136	17.276813
140	2.650	2.000	-40.097998	19.245908
110	2.625	1.200	-40.069748	36.972783
120	2.625	1.200	-40.074068	34.261983
130	2.625	1.200	-40.074482	34.002198

140	2.625	1.200	-40.071719	35.735981
110	2.625	1.400	-40.091221	23.498476
120	2.625	1.400	-40.095654	20.716768
130	2.625	1.400	-40.096132	20.416823
140	2.625	1.400	-40.093357	22.158136
110	2.625	1.600	-40.098108	19.176883
120	2.625	1.600	-40.102588	16.365683
130	2.625	1.600	-40.103062	16.068248
140	2.625	1.600	-40.100204	17.861643
110	2.625	1.800	-40.098677	18.819836
120	2.625	1.800	-40.103137	16.021186
130	2.625	1.800	-40.103533	15.772696
140	2.625	1.800	-40.100509	17.670256
110	2.625	2.000	-40.097246	19.717788
120	2.625	2.000	-40.101625	16.969966
130	2.625	2.000	-40.101881	16.809326
140	2.625	2.000	-40.098629	18.849956
110	2.600	1.200	-40.068525	37.740216
120	2.600	1.200	-40.072768	35.077733
130	2.600	1.200	-40.073101	34.868776
140	2.600	1.200	-40.070245	36.660916
110	2.600	1.400	-40.090520	23.938353
120	2.600	1.400	-40.094877	21.204336
130	2.600	1.400	-40.095272	20.956473
140	2.600	1.400	-40.092400	22.758653
110	2.600	1.600	-40.097958	19.271008
120	2.600	1.600	-40.102361	16.508126
130	2.600	1.600	-40.102747	16.265911
140	2.600	1.600	-40.099783	18.125821
110	2.600	1.800	-40.099081	18.566326
120	2.600	1.800	-40.103460	15.816503
130	2.600	1.800	-40.103763	15.628371
140	2.600	1.800	-40.100629	17.594956
110	2.600	2.000	-40.098166	19.140488
120	2.600	2.000	-40.102464	16.443493
130	2.600	2.000	-40.102624	16.343093
140	2.600	2.000	-40.099260	18.454003
110	2.600	2.200	-40.097179	19.759831
120	2.600	2.200	-40.101315	17.164491
130	2.600	2.200	-40.101321	17.160726
140	2.600	2.200	-40.097722	19.419098
110	2.500	1.200	-40.063192	41.086673
120	2.500	1.200	-40.067121	38.621226
130	2.500	1.200	-40.067114	38.625618
140	2.500	1.200	-40.063868	40.662483
110	2.500	1.400	-40.087454	25.862268
120	2.500	1.400	-40.091498	23.324658
130	2.500	1.400	-40.091546	23.294538
140	2.500	1.400	-40.088264	25.353993
110	2.500	1.600	-40.097229	19.728456
120	2.500	1.600	-40.101313	17.165746
130	2.500	1.600	-40.101335	17.151941
140	2.500	1.600	-40.097936	19.284413
110	2.500	1.800	-40.100635	17.591191
120	2.500	1.800	-40.104575	15.118841
130	2.500	1.800	-40.104611	15.096251

140	2.500	1.800	-40.100986	17.370938
110	2.500	2.000	-40.101757	16.887136
120	2.500	2.000	-40.105728	14.395333
130	2.500	2.000	-40.105508	14.533383
140	2.500	2.000	-40.101685	16.932316
110	2.500	2.200	-40.102358	16.510008
120	2.500	2.200	-40.106237	14.075936
130	2.500	2.200	-40.105868	14.307483
140	2.500	2.200	-40.101873	16.814346
110	2.500	2.400	-40.103178	15.995458
120	2.500	2.400	-40.106974	13.613468
130	2.500	2.400	-40.106476	13.925963
140	2.500	2.400	-40.102294	16.550168
110	2.500	2.600	-40.104235	15.332191
120	2.500	2.600	-40.107974	12.985968
130	2.500	2.600	-40.107382	13.357448
140	2.500	2.600	-40.103052	16.074523
110	2.500	2.800	-40.105470	14.557228
120	2.500	2.800	-40.109174	12.232968
130	2.500	2.800	-40.108521	12.642726
140	2.500	2.800	-40.104039	15.455181
110	2.500	3.000	-40.106594	13.851918
120	2.500	3.000	-40.110288	11.533933
130	2.500	3.000	-40.109605	11.962516
140	2.500	3.000	-40.105070	14.808228
110	2.500	3.200	-40.107597	13.222536
120	2.500	3.200	-40.111292	10.903923
130	2.500	3.200	-40.110598	11.339409
140	2.500	3.200	-40.106036	14.202063
110	2.500	3.400	-40.108441	12.692926
120	2.500	3.400	-40.112145	10.368666
130	2.500	3.400	-40.111451	10.804151
140	2.500	3.400	-40.106877	13.674336
110	2.500	3.600	-40.109122	12.265598
120	2.500	3.600	-40.112838	9.933808
130	2.500	3.600	-40.112151	10.364901
140	2.500	3.600	-40.107576	13.235713
110	2.500	3.800	-40.109653	11.932396
120	2.500	3.800	-40.113297	9.645786
130	2.500	3.800	-40.112706	10.016636
140	2.500	3.800	-40.108135	12.884941
110	2.500	4.000	-40.110056	11.679513
120	2.500	4.000	-40.113800	9.330153
130	2.500	4.000	-40.113134	9.748068
140	2.500	4.000	-40.108570	12.611978
110	2.500	5.000	-40.110909	11.144256
120	2.500	5.000	-40.114701	8.764776
130	2.500	5.000	-40.114077	9.156336
140	2.500	5.000	-40.109549	11.997656
110	2.500	6.000	-40.110991	11.092801
120	2.500	6.000	-40.114799	8.703281
130	2.500	6.000	-40.114191	9.084801
140	2.500	6.000	-40.109677	11.917336
110	2.500	10.000	-40.110915	11.140491
120	2.500	10.000	-40.114726	8.749088
130	2.500	10.000	-40.114121	9.128726

140	2.500	10.000	-40.109610	11.959378
110	2.500	100.000	-40.110915	11.140491
120	2.500	100.000	-40.114726	8.749088
130	2.500	100.000	-40.114121	9.128726
140	2.500	100.000	-40.109610	11.959378
110	2.400	1.200	-40.056995	44.975291
120	2.400	1.200	-40.060600	42.713153
130	2.400	1.200	-40.060236	42.941563
140	2.400	1.200	-40.056575	45.238841
110	2.400	1.400	-40.083801	28.154526
120	2.400	1.400	-40.087523	25.818971
130	2.400	1.400	-40.087207	26.017261
140	2.400	1.400	-40.083491	28.349051
110	2.400	1.600	-40.096091	20.442551
120	2.400	1.600	-40.099849	18.084406
130	2.400	1.600	-40.099496	18.305913
140	2.400	1.600	-40.095645	20.722416
110	2.400	1.800	-40.101839	16.835681
120	2.400	1.800	-40.105557	14.502636
130	2.400	1.800	-40.105098	14.790658
140	2.400	1.800	-40.101044	17.334543
110	2.400	2.000	-40.104942	14.888548
120	2.400	2.000	-40.108585	12.602566
130	2.400	2.000	-40.107983	12.980321
140	2.400	2.000	-40.103699	15.668531
110	2.400	2.200	-40.107102	13.533148
120	2.400	2.200	-40.110659	11.301131
130	2.400	2.200	-40.109913	11.769246
140	2.400	2.200	-40.105411	14.594251
110	2.400	2.400	-40.109056	12.307013
120	2.400	2.400	-40.112597	10.085036
130	2.400	2.400	-40.111723	10.633471
140	2.400	2.400	-40.106989	13.604056
110	2.400	2.600	-40.110895	11.153041
120	2.400	2.600	-40.114324	9.001343
130	2.400	2.600	-40.113372	9.598723
140	2.400	2.600	-40.108559	12.618881
110	2.400	2.800	-40.112588	10.090683
120	2.400	2.800	-40.115977	7.964086
130	2.400	2.800	-40.114980	8.589703
140	2.400	2.800	-40.110139	11.627431
110	2.400	3.000	-40.114077	9.156336
120	2.400	3.000	-40.117515	6.998991
130	2.400	3.000	-40.116478	7.649708
140	2.400	3.000	-40.111524	10.758343
110	2.400	3.200	-40.115328	8.371333
120	2.400	3.200	-40.118752	6.222773
140	2.400	3.200	-40.089184	24.776693
110	2.400	3.400	-40.116339	7.736931
120	2.400	3.400	-40.119733	5.607196
130	2.400	3.400	-40.118683	6.266071
140	2.400	3.400	-40.113715	9.383491
110	2.400	3.600	-40.117148	7.229283
120	2.400	3.600	-40.120554	5.092018
130	2.400	3.600	-40.119510	5.747128
140	2.400	3.600	-40.114514	8.882118

110	2.400	3.800	-40.117736	6.860313
120	2.400	3.800	-40.121155	4.714891
130	2.400	3.800	-40.120120	5.364353
140	2.400	3.800	-40.115138	8.490558
110	2.400	4.000	-40.118189	6.576056
120	2.400	4.000	-40.121621	4.422476
130	2.400	4.000	-40.120595	5.066291
140	2.400	4.000	-40.115616	8.190613
110	2.400	5.000	-40.119128	5.986833
120	2.400	5.000	-40.122604	3.805643
140	2.400	5.000	-40.116664	7.532993
110	2.400	6.000	-40.119220	5.929103
120	2.400	6.000	-40.122713	3.737246
140	2.400	6.000	-40.116801	7.447026
110	2.400	10.000	-40.119143	5.977421
120	2.400	10.000	-40.122639	3.783681
130	2.400	10.000	-40.121671	4.391101
140	2.400	10.000	-40.116735	7.488441
110	2.400	100.000	-40.119144	5.976793
120	2.400	100.000	-40.122639	3.783681
130	2.400	100.000	-40.121671	4.391101
140	2.400	100.000	-40.116735	7.488441
110	2.300	1.200	-40.049644	49.588043
120	2.300	1.200	-40.052924	47.529843
130	2.300	1.200	-40.052198	47.985408
140	2.300	1.200	-40.048105	50.553766
110	2.300	1.400	-40.079241	31.015926
120	2.300	1.400	-40.082642	28.881798
130	2.300	1.400	-40.081957	29.311636
140	2.300	1.400	-40.077796	31.922663
110	2.300	1.600	-40.094185	21.638566
120	2.300	1.600	-40.097613	19.487496
130	2.300	1.600	-40.096883	19.945571
140	2.300	1.600	-40.092573	22.650096
110	2.300	1.800	-40.102274	16.562718
120	2.300	1.800	-40.105663	14.436121
130	2.300	1.800	-40.104820	14.965103
140	2.300	1.800	-40.100303	17.799521
110	2.300	2.000	-40.107290	13.415178
120	2.300	2.000	-40.110603	11.336271
130	2.300	2.000	-40.109622	11.951848
140	2.300	2.000	-40.104881	14.926826
110	2.300	2.200	-40.110968	11.107233
120	2.300	2.200	-40.114198	9.080408
130	2.300	2.200	-40.113073	9.786346
140	2.300	2.200	-40.108119	12.894981
110	2.300	2.400	-40.113978	9.218458
120	2.300	2.400	-40.117140	7.234303
130	2.300	2.400	-40.115904	8.009893
140	2.300	2.400	-40.110778	11.226458
110	2.300	2.600	-40.116540	7.610803
120	2.300	2.600	-40.119656	5.655513
130	2.300	2.600	-40.118341	6.480676
140	2.300	2.600	-40.113095	9.772541
110	2.300	2.800	-40.118714	6.246618
120	2.300	2.800	-40.121802	4.308898

130	2.300	2.800	-40.120437	5.165436
110	2.300	3.000	-40.120517	5.115236
120	2.300	3.000	-40.123594	3.184418
130	2.300	3.000	-40.122200	4.059153
140	2.300	3.000	-40.116825	7.431966
110	2.300	3.200	-40.121974	4.200968
120	2.300	3.200	-40.125051	2.270151
130	2.300	3.200	-40.123645	3.152416
140	2.300	3.200	-40.118242	6.542798
110	2.300	3.400	-40.123122	3.480598
120	2.300	3.400	-40.126205	1.546016
130	2.300	3.400	-40.124796	2.430163
140	2.300	3.400	-40.119381	5.828076
110	2.300	3.600	-40.124005	2.926516
120	2.300	3.600	-40.127098	.985658
130	2.300	3.600	-40.125694	1.866668
110	2.300	3.800	-40.124672	2.507973
120	2.300	3.800	-40.127775	.560841
140	2.300	3.800	-40.120962	4.835998
130	2.300	3.800	-40.126379	1.436831
110	2.300	4.000	-40.125165	2.198616
120	2.300	4.000	-40.128280	.243953
130	2.300	4.000	-40.126892	1.114923
140	2.300	4.000	-40.121481	4.510326
110	2.300	5.000	-40.126171	1.567351
120	2.300	5.000	-40.129327	-.413039
130	2.300	5.000	-40.127976	.434713
140	2.300	5.000	-40.122595	3.811291
110	2.300	6.000	-40.126271	1.504601
120	2.300	6.000	-40.129443	-.485829
130	2.300	6.000	-40.128105	.353766
140	2.300	6.000	-40.122738	3.721558
110	2.300	10.000	-40.126195	1.552291
120	2.300	10.000	-40.129371	-.440649
130	2.300	10.000	-40.128038	.395808
140	2.300	10.000	-40.122674	3.761718
110	2.300	100.000	-40.126195	1.552291
120	2.300	100.000	-40.129371	-.440649
130	2.300	100.000	-40.128038	.395808
140	2.300	100.000	-40.122674	3.761718
110	2.200	1.200	-40.040724	55.165343
120	2.200	1.200	-40.043690	53.324178
130	2.200	1.200	-40.042608	54.003133
140	2.200	1.200	-40.038083	56.842571
110	2.200	1.400	-40.073319	34.731981
120	2.200	1.400	-40.076408	32.793633
130	2.200	1.400	-40.075362	33.449998
140	2.200	1.400	-40.070757	36.339636
110	2.200	1.600	-40.090999	23.637781
120	2.200	1.600	-40.094111	21.685001
130	2.200	1.600	-40.093005	22.379016
140	2.200	1.600	-40.088237	25.370936
110	2.200	1.800	-40.101396	17.113663
120	2.200	1.800	-40.104468	15.185983
130	2.200	1.800	-40.103248	15.951533
140	2.200	1.800	-40.098272	19.073973

110	2.200	2.000	-40.108246	12.815288
120	2.200	2.000	-40.111244	10.934043
130	2.200	2.000	-40.109886	11.786188
140	2.200	2.000	-40.104686	15.049188
110	2.200	2.200	-40.113214	9.697868
120	2.200	2.200	-40.116138	7.863058
130	2.200	2.200	-40.114655	8.793641
140	2.200	2.200	-40.109316	12.143863
110	2.200	2.400	-40.117257	7.160886
120	2.200	2.400	-40.120111	5.370001
130	2.200	2.400	-40.118517	6.370236
140	2.200	2.400	-40.112964	9.854743
110	2.200	2.600	-40.120419	5.176731
120	2.200	2.600	-40.123229	3.413456
130	2.200	2.600	-40.121560	4.460753
140	2.200	2.600	-40.115958	7.976008
110	2.200	2.800	-40.123062	3.518248
120	2.200	2.800	-40.125843	1.773171
130	2.200	2.800	-40.124122	2.853098
140	2.200	2.800	-40.118433	6.422946
110	2.200	3.000	-40.125187	2.184811
120	2.200	3.000	-40.127956	.447263
130	2.200	3.000	-40.126207	1.544761
140	2.200	3.000	-40.120456	5.153513
110	2.200	3.200	-40.126865	1.131866
120	2.200	3.200	-40.129632	-.604427
130	2.200	3.200	-40.127870	.501228
140	2.200	3.200	-40.122080	4.134453
110	2.200	3.400	-40.128168	.314233
120	2.200	3.400	-40.130934	-1.421432
130	2.200	3.400	-40.129169	-.313894
140	2.200	3.400	-40.123357	3.333136
110	2.200	3.600	-40.129148	-.300717
120	2.200	3.600	-40.131943	-2.054579
130	2.200	3.600	-40.130180	-.948297
140	2.200	3.600	-40.124342	2.715048
110	2.200	3.800	-40.129883	-.761929
120	2.200	3.800	-40.132672	-2.512027
130	2.200	3.800	-40.130916	-1.410137
140	2.200	3.800	-40.125090	2.245678
110	2.200	4.000	-40.130430	-1.105172
120	2.200	4.000	-40.133229	-2.861544
130	2.200	4.000	-40.131480	-1.764047
140	2.200	4.000	-40.125648	1.895533
110	2.200	5.000	-40.131508	-1.781617
120	2.200	5.000	-40.134344	-3.561207
130	2.200	5.000	-40.132628	-2.484417
140	2.200	5.000	-40.126823	1.158221
110	2.200	6.000	-40.131614	-1.848132
120	2.200	6.000	-40.134466	-3.637762
130	2.200	6.000	-40.132766	-2.571012
140	2.200	6.000	-40.126971	1.065351
110	2.200	10.000	-40.131539	-1.801069
120	2.200	10.000	-40.134395	-3.593209
130	2.200	10.000	-40.132696	-2.527087
140	2.200	10.000	-40.126907	1.105511

110	2.200	100.000	-40.131539	-1.801069
120	2.200	100.000	-40.134395	-3.593209
130	2.200	100.000	-40.132696	-2.527087
140	2.200	100.000	-40.126907	1.105511
110	2.100	1.200	-40.029660	62.128003
120	2.100	1.200	-40.032332	60.451323
130	2.100	1.200	-40.030914	61.341118
140	2.100	1.200	-40.025970	64.443478
110	2.100	1.400	-40.065417	39.690486
120	2.100	1.400	-40.068209	37.938506
130	2.100	1.400	-40.066813	38.814496
140	2.100	1.400	-40.061771	41.978351
110	2.100	1.600	-40.085840	26.875053
120	2.100	1.600	-40.088654	25.109268
130	2.100	1.600	-40.087195	26.024791
140	2.100	1.600	-40.081984	29.294693
110	2.100	1.800	-40.098492	18.935923
120	2.100	1.800	-40.101262	17.197748
130	2.100	1.800	-40.099685	18.187316
140	2.100	1.800	-40.094265	21.588366
110	2.100	2.000	-40.107081	13.546326
120	2.100	2.000	-40.109775	11.855841
130	2.100	2.000	-40.108061	12.931376
140	2.100	2.000	-40.102429	16.465456
110	2.100	2.200	-40.113386	9.589938
120	2.100	2.200	-40.116003	7.947771
130	2.100	2.200	-40.114162	9.102998
140	2.100	2.200	-40.108343	12.754421
110	2.100	2.400	-40.118258	6.532758
120	2.100	2.400	-40.120811	4.930751
130	2.100	2.400	-40.118867	6.150611
140	2.100	2.400	-40.112698	9.896158
110	2.100	2.600	-40.122110	4.115628
120	2.100	2.600	-40.124617	2.542486
130	2.100	2.600	-40.122599	3.808781
140	2.100	2.600	-40.116520	7.623353
110	2.100	2.800	-40.125166	2.197988
120	2.100	2.800	-40.127645	.642416
130	2.100	2.800	-40.125577	1.940086
140	2.100	2.800	-40.119423	5.801721
110	2.100	3.000	-40.127570	.689478
120	2.100	3.000	-40.130035	-.857309
130	2.100	3.000	-40.127939	.457931
140	2.100	3.000	-40.121737	4.349686
110	2.100	3.200	-40.129436	-.481437
120	2.100	3.200	-40.131897	-2.025714
130	2.100	3.200	-40.129786	-.701062
140	2.100	3.200	-40.123556	3.208263
110	2.100	3.400	-40.130860	-1.374997
120	2.100	3.400	-40.133324	-2.921157
130	2.100	3.400	-40.131208	-1.593367
140	2.100	3.400	-40.124964	2.324743
110	2.100	3.600	-40.131931	-2.047049
120	2.100	3.600	-40.134400	-3.596347
130	2.100	3.600	-40.132286	-2.269812
140	2.100	3.600	-40.126036	1.652063

110	2.100	3.800	-40.132722	-2.543402
120	2.100	3.800	-40.135200	-4.098347
130	2.100	3.800	-40.133090	-2.774322
140	2.100	3.800	-40.126841	1.146926
110	2.100	4.000	-40.133300	-2.906097
120	2.100	4.000	-40.135786	-4.466062
130	2.100	4.000	-40.133682	-3.145802
140	2.100	4.000	-40.127436	.773563
110	2.100	5.000	-40.134445	-3.624584
120	2.100	5.000	-40.136964	-5.205257
130	2.100	5.000	-40.134889	-3.903194
140	2.100	5.000	-40.128667	.001111
110	2.100	6.000	-40.134555	-3.693609
120	2.100	6.000	-40.137089	-5.283694
130	2.100	6.000	-40.135028	-3.990417
140	2.100	6.000	-40.128818	-.093642
110	2.100	10.000	-40.134480	-3.646547
120	2.100	10.000	-40.137019	-5.239769
130	2.100	10.000	-40.134961	-3.948374
140	2.100	10.000	-40.128755	-.054109
110	2.100	100.000	-40.134480	-3.646547
120	2.100	100.000	-40.137019	-5.239769
130	2.100	100.000	-40.134961	-3.948374
140	2.100	100.000	-40.128755	-.054109
110	2.060	1.200	-40.024467	65.386611
120	2.060	1.200	-40.027033	63.776446
130	2.060	1.200	-40.025487	64.746561
140	2.060	1.200	-40.020378	67.952458
120	2.060	1.400	-40.064195	40.457291
130	2.060	1.400	-40.062669	41.414856
110	2.060	1.600	-40.083033	28.636446
120	2.060	1.600	-40.085733	26.942196
130	2.060	1.600	-40.084138	27.943058
110	2.060	1.800	-40.096566	20.144488
120	2.060	1.800	-40.099219	18.479731
130	2.060	1.800	-40.097505	19.555266
140	2.060	1.800	-40.091915	23.062991
110	2.060	2.000	-40.105822	14.336348
120	2.060	2.000	-40.108399	12.719281
130	2.060	2.000	-40.106547	13.881411
110	2.060	2.200	-40.112612	10.075623
120	2.060	2.200	-40.115111	8.507501
130	2.060	2.200	-40.113133	9.748696
110	2.060	2.400	-40.117826	6.803838
120	2.060	2.400	-40.120260	5.276503
130	2.060	2.400	-40.118180	6.581703
110	2.060	2.600	-40.121915	4.237991
120	2.060	2.600	-40.124303	2.739521
130	2.060	2.600	-40.122149	4.091156
140	2.060	2.600	-40.115909	8.006756
110	2.060	2.800	-40.125134	2.218068
120	2.060	2.800	-40.127494	.737168
130	2.060	2.800	-40.125290	2.120178
140	2.060	2.800	-40.118976	6.082213
110	2.060	3.000	-40.127650	.639278
120	2.060	3.000	-40.129995	-.832209

110	2.060	3.200	-40.129592	-.579327
120	2.060	3.200	-40.131932	-2.047677
130	2.060	3.200	-40.129684	-.637057
110	2.060	3.400	-40.131069	-1.506144
120	2.060	3.400	-40.133411	-2.975749
130	2.060	3.400	-40.131157	-1.561364
140	2.060	3.400	-40.124753	2.457146
110	2.060	3.600	-40.132174	-2.199532
120	2.060	3.600	-40.134522	-3.672902
130	2.060	3.600	-40.132269	-2.259144
140	2.060	3.600	-40.125859	1.763131
110	2.060	3.800	-40.132990	-2.711572
120	2.060	3.800	-40.135345	-4.189334
130	2.060	3.800	-40.133096	-2.778087
140	2.060	3.800	-40.126685	1.244816
110	2.060	4.000	-40.133583	-3.083679
120	2.060	4.000	-40.135946	-4.566462
130	2.060	4.000	-40.133702	-3.158352
140	2.060	4.000	-40.127295	.862041
110	2.060	5.000	-40.134753	-3.817854
120	2.060	5.000	-40.137147	-5.320089
130	2.060	5.000	-40.134931	-3.929549
140	2.060	5.000	-40.128546	.077038
110	2.060	6.000	-40.134867	-3.889389
120	2.060	6.000	-40.137275	-5.400409
130	2.060	6.000	-40.135004	-3.975357
140	2.060	6.000	-40.128698	-.018342
110	2.060	10.000	-40.134790	-3.841072
120	2.060	10.000	-40.137203	-5.355229
130	2.060	10.000	-40.135004	-3.975357
140	2.060	10.000	-40.128634	.021818
110	2.060	100.000	-40.134790	-3.841072
120	2.060	100.000	-40.137203	-5.355229
130	2.060	100.000	-40.135004	-3.975357
140	2.060	100.000	-40.128634	.021818
110	2.000	1.200	-40.015660	70.913003
120	2.000	1.200	-40.018078	69.395708
130	2.000	1.200	-40.016355	70.476891
140	2.000	1.200	-40.011015	73.827741
110	2.000	1.400	-40.054658	46.441758
120	2.000	1.400	-40.057186	44.855438
130	2.000	1.400	-40.055471	45.931601
140	2.000	1.400	-40.050021	49.351476
110	2.000	1.600	-40.077813	31.911996
120	2.000	1.600	-40.080351	30.319401
130	2.000	1.600	-40.078560	31.443253
140	2.000	1.600	-40.072933	34.974196
110	2.000	1.800	-40.092642	22.606798
120	2.000	1.800	-40.095126	21.048088
130	2.000	1.800	-40.093212	22.249123
140	2.000	1.800	-40.087375	25.911841
110	2.000	2.000	-40.102871	16.188101
120	2.000	2.000	-40.105277	14.678336
130	2.000	2.000	-40.103223	15.967221
140	2.000	2.000	-40.097180	19.759203
110	2.000	2.200	-40.110364	11.486243

120	2.000	2.200	-40.112691	10.026051
130	2.000	2.200	-40.110512	11.393373
140	2.000	2.200	-40.104286	15.300188
110	2.000	2.400	-40.116073	7.903846
120	2.000	2.400	-40.118334	6.485068
130	2.000	2.400	-40.116053	7.916396
140	2.000	2.400	-40.109683	11.913571
110	2.000	2.600	-40.120506	5.122138
120	2.000	2.600	-40.122720	3.732853
130	2.000	2.600	-40.120365	5.210616
140	2.000	2.600	-40.113889	9.274306
110	2.000	2.800	-40.123962	2.953498
120	2.000	2.800	-40.126146	1.583038
130	2.000	2.800	-40.123741	3.092176
140	2.000	2.800	-40.117192	7.201673
110	2.000	3.000	-40.126641	1.272426
120	2.000	3.000	-40.128809	-.087994
130	2.000	3.000	-40.126374	1.439968
140	2.000	3.000	-40.119778	5.578958
110	2.000	3.200	-40.128694	-.015832
120	2.000	3.200	-40.130857	-1.373114
130	2.000	3.200	-40.128406	.164888
140	2.000	3.200	-40.121781	4.322076
110	2.000	3.400	-40.130247	-.990339
120	2.000	3.400	-40.132409	-2.346994
130	2.000	3.400	-40.129953	-.805854
140	2.000	3.400	-40.123312	3.361373
110	2.000	3.600	-40.131404	-1.716357
120	2.000	3.600	-40.133571	-3.076149
130	2.000	3.600	-40.131114	-1.534382
140	2.000	3.600	-40.124467	2.636611
110	2.000	3.800	-40.132254	-2.249732
120	2.000	3.800	-40.134427	-3.613289
130	2.000	3.800	-40.131973	-2.073404
140	2.000	3.800	-40.125326	2.097588
110	2.000	4.000	-40.132870	-2.636272
120	2.000	4.000	-40.135050	-4.004222
130	2.000	4.000	-40.132601	-2.467474
140	2.000	4.000	-40.125956	1.702263
110	2.000	5.000	-40.134076	-3.393037
120	2.000	5.000	-40.136285	-4.779184
130	2.000	5.000	-40.133861	-3.258124
140	2.000	5.000	-40.127235	.899691
110	2.000	6.000	-40.134187	-3.462689
120	2.000	6.000	-40.136415	-4.860759
130	2.000	6.000	-40.134002	-3.346602
140	2.000	6.000	-40.127388	.803683
110	2.000	10.000	-40.134114	-3.416882
120	2.000	10.000	-40.136341	-4.814324
130	2.000	10.000	-40.133934	-3.303932
140	2.000	10.000	-40.127323	.844471
110	2.000	100.000	-40.134114	-3.416882
120	2.000	100.000	-40.136341	-4.814324
130	2.000	100.000	-40.133934	-3.303932
140	2.000	100.000	-40.127323	.844471

TECHNICAL INFORMATION DIVISION
LAWRENCE BERKELEY LABORATORY
UNIVERSITY OF CALIFORNIA
BERKELEY, CALIFORNIA 94720